

The Expanding Envelope of Supernova 1987A in the Large Magellanic Cloud

R. W. Hanuschik

Astronomisches Institut, Ruhr-Universität Bochum,
Postfach 1021 48, W-4630 Bochum 1, Fed. Rep. of Germany

1. Introduction

The Ludwig Biermann Award 1990 of the Astronomische Gesellschaft clearly is not only a distinction for me and my collaborators in the Bochum SN 1987A project, but also an excellent opportunity to express my thanks to the Bochum Institute Director, Prof. Theodor Schmidt-Kaler, who invested a lot of time and dedication in this programme. In fact this work would have been impossible without his permanent and inspiring support in the background.

Supernovae indicate the explosive end of a star. With a mean absolute brightness at maximum of $M_b = -19.0$ (type Ia), -17.1 (type Ib), and -16.9 (type II; Miller and Branch, 1990), they are the intrinsically brightest single objects in the sky. Type-II SNe are the most energetic (albeit not the most luminous) ones. They release a total energy of $\sim 10^{53}$ erg, most of which is emitted *within seconds* after core collapse (Burrows, 1988) in form of neutrinos. (For comparison, the Sun emits 10^{51} erg in 10^{10} years).

Meanwhile, supernovae are frequently observed objects. The Asiago Supernova Catalogue (Barbon *et al.*, 1989) lists 661 extragalactic objects. Automatic survey programmes like the Berkeley Automated Supernova Search (Kare *et al.*, 1989), are now inflating this list dramatically. By October 29, 1990 (IAU *Circular* 5124), 32 supernovae have been discovered this year. Prospects are good that soon the discovery rate will increase to one SN per night (Perlmutter, 1990).

Most of these supernova detections, however, are only valuable for improving supernova statistics. For understanding the physics of the explosion, a nearby supernova is needed, and these are rare. Only five galactic SNe have been observed this millenium, and none of them by telescope. This is the reason why SN 1987A in the LMC immediately caused restless activity at all southern observatories. It was by far the brightest extragalactic supernova in historical times, and by far the brightest supernova since the invention of the telescope. It is now the probably best investigated (although not best understood) extra-solar system object in astronomy, with more than 1230 papers dealing with it in 1987-89 (as counted from the *A&A Abstracts*).

2. What we have seen: collapse and explosion

Nowadays supernovae are classified according to their spectra, not to their lightcurve which is thought of as being only a secondary criterion for classification (Filippenko, 1990). Type-I's do not show Balmer lines, type-II's do. The physical reason therefore are the different progenitor histories: type-II SNe arise from evolved single massive stars with large hydrogen envelopes, while type-I progenitors supposedly are white dwarfs in evolved binary systems or exploding WR stars, with little, if any, hydrogen. SN 1987A, as a type-II event, was caused by the *collapse* of the $\approx 1.4 M_{\odot}$ iron core of its $\approx 20 M_{\odot}$ progenitor, releasing the binding energy $GM^2/R \sim 2-3 \cdot 10^{53}$ erg mostly in a neutrino/anti-neutrino burst. This event is the only information we have about the physics of the collapse.

The subsequent shock wave running through the envelope finally reached the surface and caused the brightening of the supernova. The energy of this *explosion*, mostly in form of mechanical energy, is only a small fraction of the collapse energy, $\sim 1\%$, and the electromagnetic energy, the primary source of information about the explosion, is again only $\sim 1\%$ of the kinetic energy. Peering at the photons from SN 1987A, we are thus watching a phenomenon subordinate in terms of energy, but highly informative: the *perfume*.

Canonical progenitors of type-II SNe are red supergiants. The progenitor of SN 1987A, the first one ever really observed, was a blue supergiant. This is already implied by the fact that the time required for the shock wave to traverse the extended ($\sim 10^{14}$ cm) envelope of a red supergiant would be days, not hours as observed. Thus the progenitor must have been a comparatively "compact" object, i.e. a blue supergiant.

Serendipitous *observations* of the progenitor started in the early 1970's when Sanduleak (1969) took objective prism spectra of OB-type stars in the LMC, among them Sk -69° 202. Isserstedt (1975) proved wise foresight when he performed photoelectric photometry on the Sanduleak star in 1971-73. Spectrograms exist from 1972 (Walborn *et al.*, 1989) and 1977 (González *et al.*, 1987). The next two important time points both occurred on February 23, 1987: at $t_0 = 23.316$ UT, a total number of 19 neutrinos from the core collapse of Sk -69° 202 were registered in the Kamioka and IMB detectors (Hirata *et al.*, 1987; Bionta *et al.*, 1987), and $\Delta t = 2.41 \pm 0.64$ hours later, on $t_1 = 23.390 \dots 23.443$ UT, photons from the explosion arrived on Earth. This time point is fixed by the non-detection of SN 1987A by the amateur astronomer Jones, and the first positive detection on a photographic plate.

This review, as necessarily all others on SN 1987A, does not intend to be comprehensive, not even concerning the observational facts, and by no means with regard to the theoretical progress in understanding these observ-

ations. The diligent reader must instead be referred to the conference proceedings hitherto dedicated to SN 1987A, i.e. the ESO 1987 and 1990 conferences (Danziger, 1987, 1990), the 1987 George Mason Workshop (Kafatos and Michalitsianos, 1988), the 1988 La Thuile Workshop (Greco, 1988), the 1988 White Conference (Proust and Couch, 1988) and the 1989 Santa Cruz Workshop (Woosley, 1990). Recent reviews are, e.g., by Dopita (1988), Arnett *et al.* (1989), McCray (1989) and Hillebrandt and Höflich (1989).

Spectroscopic observations of the explosion started on February 24.8 with the IUE satellite (e.g., Wamsteker *et al.*, 1987; Kirshner *et al.*, 1987) and at the South African Observatory (Menzies *et al.*, 1987). Slightly later the Chilean observatories took over (ESO, CTIO, Bochum telescope). At that time, the supernova was at $V \approx 5^m$, and small telescopes were favoured in the observations. The smallest and least efficient of them could do the best job: the 61cm telescope of the Ruhr-Universität Bochum on La Silla, equipped with a rapid spectrum scanner spectrograph (Haupt *et al.*, 1976) and a photomultiplier. (This telescope has already a good tradition in observing what we now call SN 1987A: Isserstedt [1975] performed his 1971–73 photometry at the Bochum telescope.) With its large entrance slit (20–30"), it is ideally suited for performing precise spectrophotometry of bright ($V < 7^m$) objects. Observers in the Bochum SN 1987A campaign are listed in Table 1.

The scanner spectrograph was used until day 314 (1988 January 3); observations could be continued, albeit at lower accuracy, with a different detector (OMA, kindly provided by Prof. Geyer from Hoher List Observatory) until day 450. At present, data for the first 314 days are fully re-

Tab. 1: List of observers in the Bochum SN 1987A program

Time of observation	Days ^a	Observer
25. 2. – 15. 3. 1987.....	1.7–20	J. Dachs
16. 3. – 15. 4. 1987.....	21–50	R. Hanuschik
16. 4. – 14. 6. 1987.....	51–111	G. Thimm
15. 6. – 30. 7. 1987.....	112–157	K. Seidensticker
31. 7. – 10. 9. 1987.....	158–198	J. Gochermann
11. 9. – 15.11. 1987.....	199–265	S. Kimeswenger
16.11. – 15.12. 1987.....	266–293	R. Poetzal
16.12. – 3. 1. 1988.....	294–314	G. Schnur
4. 1. – 20. 2. 1988.....	315–362	U. Lemmer
21. 2. – 30. 4. 1988.....	363–432	J. Stüwe
30. 4. – 17. 5. 1988.....	433–449	M. Werger

^a Days since 23.316 February 1987 (UT)

duced. They usually cover the wavelength range 3 200–8 700 Å at a resolution of 10, later 15 Å. Most spectral regions have been additionally measured at 3–5 Å resolution and fluxed with the spectrophotometry. Flux calibration was performed with flux standard stars from the list of Tüg (1980a, b). Accuracy of the flux scale is 3 %, slightly worse at the corners of the spectra. The Bochum spectrophotometric atlas of SN 1987A therefore represents the *fully resolved, precisely calibrated, quasi-continuous time-record of the optical evolution of an expanding supernova envelope*. The reduced part of this data set is published or will be published soon (Hanuschik and Dachs, 1988; Hanuschik *et al.*, 1989, 1991) and is available upon request on magnetic tape.

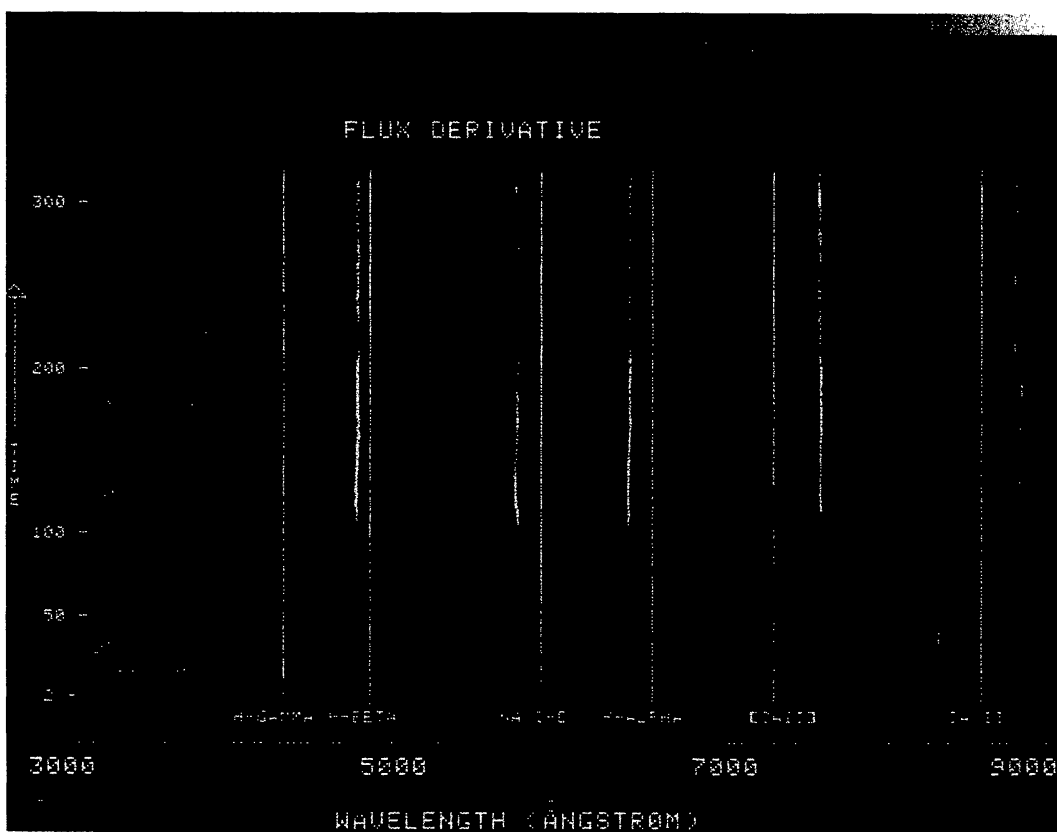
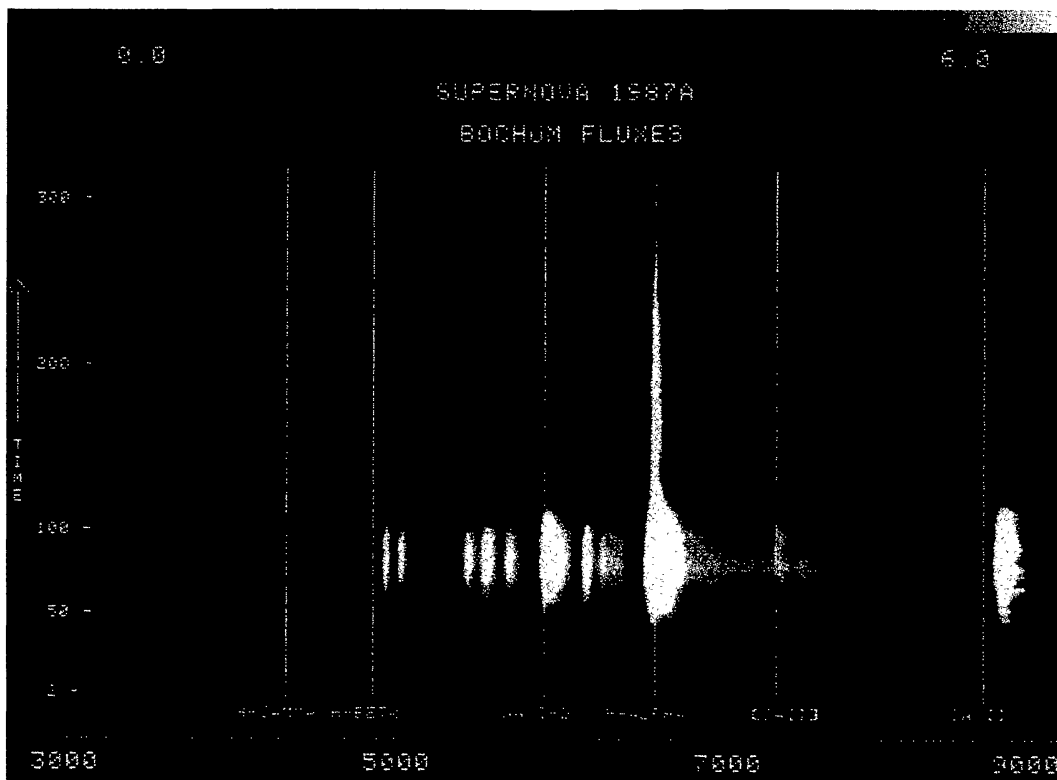
In the following, I will focus on recent and interesting results about the energetics in the expanding envelope (chapter 3), the evolution of the flux in the lines (chapter 4), mixing and clumping processes (chapter 5) and about the surrounding circumstellar medium (chapter 6). Other aspects, like kinematics, distance determination and the *Bochum event*, are reviewed in more detail in Hanuschik (1989, 1990a).

3. Bolometric luminosity and energetics

3.1 Overview over the spectrum

Figure 1 shows the colour-coded evolution of the optical spectrum of SN 1987A, and of its first derivative. The flux record shows best the brightness evolution, as well as the change from a rather blue, hot spectrum into a red, cool spectrum during the first few days. The flux derivative demonstrates the evolution of the line spectrum and especially emphasizes the kinematics.

Some momentary shots of the spectral evolution of SN 1987A, as seen from the Bochum telescope, are shown in Fig. 2. While essentially a black body with few, extremely broad hydrogen and helium lines on day 2 (Feb. 25), the optical spectrum evolves quickly into one with strong absorption lines, and finally an emission-line dominated nebular-type spectrum around day 300. This transition from a stellar into a nebular spectrum is essentially caused by the different evolution of continuum- and line-forming regions in the expanding envelope. Initially, photosphere and atmosphere are close together, frozen in the expanding matter. After 5 days, the photosphere starts falling back in comoving frame (but still expands for the observer), while the line-forming regions keep on expanding. After day 100, the photosphere shrinks, and most light is emitted in the lines.



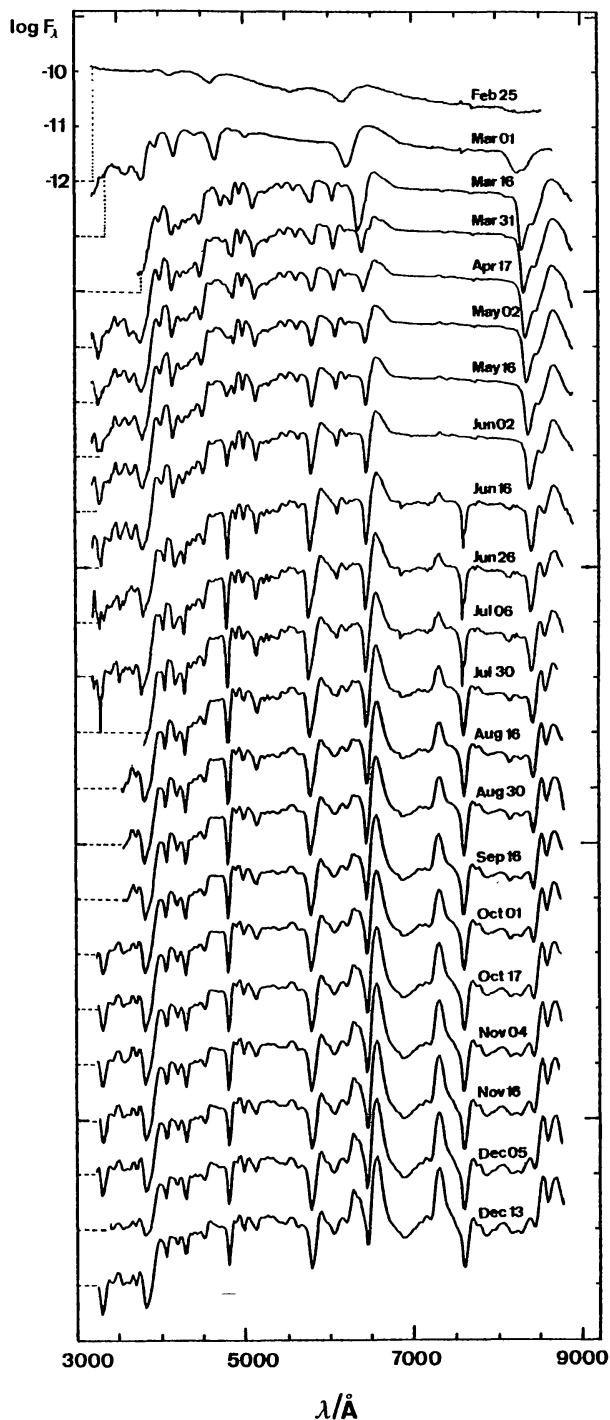


Fig. 2: Selected spectra of SN 1987A. Logarithmic flux scale is in $\text{erg s}^{-1}\text{cm}^{-2}\text{\AA}^{-1}$. Spectra are shifted by -1 dex each, the broken line marking $\log F = -12$. The strong absorption lines in the red after June 16 are telluric

Fig. 1 (previous page). **Top:** Colour-coded fluxes of SN 1987A as measured at the Bochum telescope. The flux scale is logarithmic. The ordinate is in days since core collapse. Rest wavelengths of a few strong lines are marked. This figure particularly emphasizes the brightness evolution, with its maximum occurring on day 82. **Bottom:** Normalized spectral derivative $[F(\lambda + \Delta\lambda) - F(\lambda)]/F(\lambda)$. Negative flux gradients appear blue-white, positive red. Green codes spectral regions with virtually constant flux across $\Delta\lambda \approx 5 \text{ \AA}$. This figure emphasizes the line spectrum, and particularly its kinematical evolution

3.2 The bolometric lightcurve

The bolometric lightcurve (BLC) of a supernova provides the record of electromagnetic energy radiated away. It is defined as

$$L_{\text{bol}}(t) = 4\pi D^2 \int_0^\infty F_\lambda d\lambda, \quad F_\lambda = F_\lambda \cdot 10^{0.4 A(\lambda) \cdot E(B-V)} \quad (1)$$

where F_λ are the measured fluxes, D is the distance, $A(\lambda)$ is the extinction law and E_{B-V} is the reddening. SN 1987A is the first supernova for which a BLC could be constructed. The hitherto derived BLCs for SN 1987A are from photometric data (Whitelock *et al.*, 1988; Dopita *et al.*, 1988; Suntzeff and Bouchet, 1990). These all suffer from intrinsic systematic errors due to calculating monochromatic fluxes from broad-band magnitudes, i.e. weighted means of the spectrum. The best way to derive the BLC therefore is to use spectrophotometry. Figure 3 shows the BLC derived from the Bochum data (Hanuschik, 1990b). This lightcurve includes 0.9–20 μ IR photometry (Bouchet *et al.*, 1989b) and therefore is not ideal, but offers a better time coverage than the truly spectrophotometric BLC of Bouchet *et al.* (1990). Its inner precision is 3 %, but the remaining uncertainties are larger: the uncertainties of the extinction towards SN 1987A, $E_{B-V} = 0.17 \pm 0.02$ (Walker and Suntzeff, 1990), results in a 4 % error in L_{bol} , but the

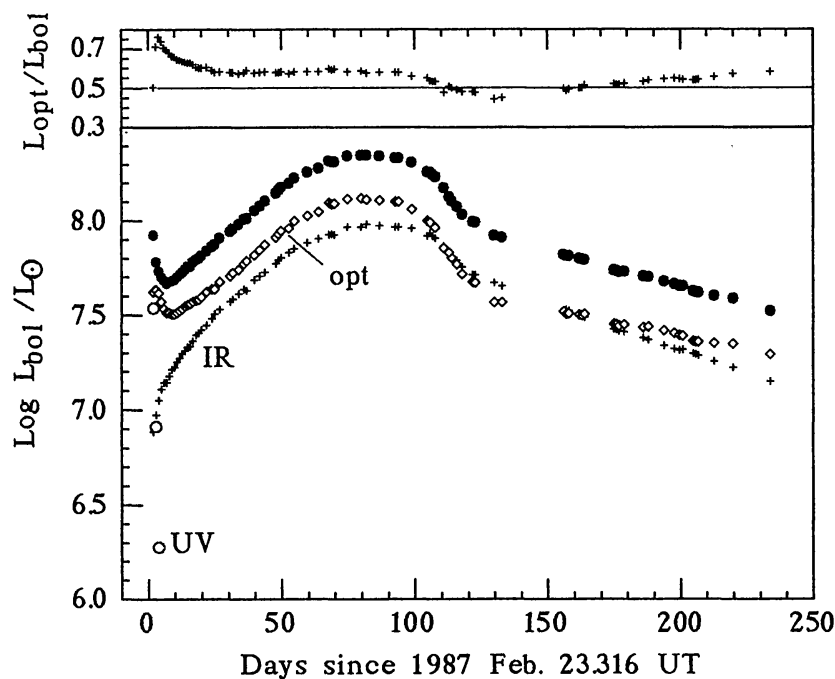


Fig. 3: The Bochum semi-spectrophotometric BLC, for $E_{B-V} = 0.16$ and $D = 50$ kpc. Besides the bolometric lightcurve (solid circles), also its contributions from the optical (diamonds), infrared (crosses) and UV (open circles) are shown. Furthermore the fraction $L_{\text{opt}}/L_{\text{bol}}$ is shown on top

largest error, 15–20 %, comes from the distance which is only known within ≈ 10 %.

As shown in Fig. 3, the optical range (0.32–0.86 μ) dominates L_{bol} throughout the investigated period except for a short phase during the steep fall-off after maximum. The IR range (0.86–20 μ) contributes only a small fraction in the initial period, later-on it rivals with the optical range. The UV range (0.12–0.32 μ) is very strong on day 2, but drops to an insignificant (< 1 %) level after day 5. This evolution demonstrates the influence of the dramatic temperature fall-off during the first ~ 10 days (see, e.g., Hanuschik 1989).

3.3 Phases of evolution

The general form of the BLC is essentially determined by the balance between the release of shock-deposited energy (thermal plus nuclear) and diffusion through the opaque envelope (e.g., McCray, 1989; Shigeyama and Nomoto, 1990). During the first 10 days, the dense *bsg* envelope effectively hinders diffusion of most of the internal energy, thereby favouring its transformation into kinetic energy while the envelope cools off adiabatically. If we simply assume that the photosphere moves with the matter, $r_{\text{ph}} \sim t$, then from a diffusion ansatz it follows that

$$L(t) \sim t^{-1}, \quad T_{\text{eff}}(t) \sim t^{-3/4} \quad (2)$$

which is quite good an approximation to the observed values. When T has dropped to ≈ 5000 K, hydrogen recombination starts, and energy is transported more efficiently than by diffusion. The photosphere now starts to recede. As a result, L increases again, at a rate

$$L(t) = \varepsilon_{\text{H}} \cdot \dot{M}_{\text{H}}(t) \quad (\varepsilon_{\text{H}} = 1.3 \cdot 10^{13} \text{ erg g}^{-1}). \quad (3)$$

From day 9 until day 21, a mass of $10 M_{\odot}$ recombining hydrogen is required to penetrate the photosphere, in order to produce the observed luminosity. As this is the estimated total hydrogen mass in the envelope of SN 1987A, luminosity should drop steeply after that date. Instead another energy source takes over: radioactive decay of nickel-56 (mother) and cobalt-56 (daughter), nucleosynthesized by the shock deep inside the core. As the envelope becomes thinner, diffusion of thermalized energy from this store becomes more and more important, dominating the lightcurve around maximum (day 82). When the store is empty, only the actually produced decay energy is radiated away, and the lightcurve finds its final, exponential decay phase,

$$L(t) = M_{\odot}({}^{56}\text{Ni}) \cdot \varepsilon_{\text{Co}} \cdot \tau_{\text{Co}}^{-1} \cdot \exp(-t/\tau_{\text{Co}}), \quad (4)$$

with $\varepsilon_{\text{Co}} = 6.4 \cdot 10^{16} \text{ erg g}^{-1}$ and $\tau_{\text{Co}} = 111.3^{\text{d}}$.

A fit to the exponential tail of the BLC yields the initially produced mass of ^{56}Ni ,

$$M_0(^{56}\text{Ni}) = (0.078 \pm 0.002) (D/50 \text{ kpc})^2 M_\odot . \quad (5)$$

During this exponential tail phase, the SN 1987A lightcurve and those of ordinary type-II SNe look similar (Phillips, 1988). They are dominated by the initial ^{56}Ni mass which is a function of the explosion energy and of processes in the interior, and therefore is not different for blue and red supergiants. In the initial phase, however, this difference is very important and caused what was called an unusual lightcurve in the case of SN 1987A: the initial shape of the lightcurve (and the maximum brightness!) is a function of how easy photons can diffuse through the envelope. A red supergiant with its tenuous envelope enables a high initial luminosity, while a blue supergiant with its dense and rather compact envelope hinders diffusion efficiently. Popping up the progenitor's radius from $3 \cdot 10^{12}$ cm (*bsg*) to $4 \cdot 10^{14}$ cm (*rsg*), hydrodynamic model calculations can smoothly transform a type-1987A lightcurve into an ordinary type-II lightcurve (Arnett, 1989).

By now, the brightness of SN 1987A has dropped by a factor of $2 \cdot 10^4$ since maximum ($L_{\text{bol}} \approx 9 \cdot 10^3 L_\odot$) and it becomes more and more difficult to measure, because contributions from background stars or light-echoes become increasingly more important. At day 1000, 80 % of the total light come from the far-IR, dominated by a ~ 100 K black body, the dust in the envelope. Bouchet *et al.* (1989a) detected a levelling-off in the lightcurve around that date, but this is not confirmed by CTIO measurements (Bouchet, 1990). Such a levelling-off would be an evidence for energy input by a central pulsar.

3.4 Energetics

The total amount of electromagnetic energy radiated away from SN 1987A is

$$E_{\text{rad}} = \int_0^\infty L_{\text{bol}}(t) dt = 9.4 \cdot 10^{48} (D/50 \text{ kpc})^2 \text{ erg} \quad (6)$$

(Hanuschik, 1990b), including contributions from Woosley's (1988) model 10H for the unobserved period day 0–1.7, and from the extrapolation of the radioactive tail from day 234 to infinity. This energy has to be compared to the total energy from the decay of $0.078 M_\odot$ nickel-56, $1.47 \cdot 10^{49}$ erg. Allowing for the fact that part of the radiated energy is due to hydrogen recombination ($2.7 \cdot 10^{47}$ erg), we find that

$$\Delta E \approx 5.6 \cdot 10^{48} \text{ erg} \quad (7)$$

from the ^{56}Ni decay has not been radiated away. Instead, this energy went presumably into thermal, kinetic and turbulent energy of the nickel bubble (e.g., Müller *et al.*, 1989; Arnett *et al.*, 1989), driving acceleration and turbulent mixing there. This energy is sufficient to accelerate the whole nickel bubble from its initial $\sim 1000 \text{ km s}^{-1}$ to 3000 km s^{-1} .

4. Troughs and humps: absorption and emission line lightcurves

4.1 Absorption lines

At first view, a supernova spectrum is completely different from a stellar one. Absorption and emission features overlap, both broadened to several 10^3 km s^{-1} , and there are wide spectral regions without any continuum. Only few features can be reliably assigned to a single or dominating transition.

The equivalent width of absorption lines, W_λ , is a measure of the integral opacity within the envelope. In general, it is a complex function of density and excitation conditions and can only be fully understood by careful modelling. Its temporal evolution is expected to follow the following trends: initially, W_λ for most optical lines is expected to increase as a result of cooling in the envelope and increasing size of the line absorbing volume above the photosphere. Subsequently, W_λ will eventually fall off again, because expansive dilution ($n \sim t^{-3}$) causes a decrease of the Sobolev optical depth, $\tau_{\text{Sob}} \sim t \cdot n \sim t^{-2}$.

Only few lines are embedded in pseudo-continuum such that their equivalent width is defined in a sufficiently reliable way. From among them, the Balmer lines $\text{H}\alpha$ and $\text{H}\beta$, and furthermore $\text{Ca II-2 } \lambda 8500$, $\text{Ba II-2 } \lambda 6141$ and the ground-state line Na I-D were selected for measuring W_λ . Figure 4 shows the results for days 2–314.

The general evolutionary scenario described above is best followed by the Ba II and the Ca II line: their absorption strength indeed shows a steep increase and a subsequent slow decrease. $\text{H}\alpha$, $\text{H}\beta$ and Na I-D troughs exhibit a more complex evolution after the initial increase of W_λ : absorption in these lines drops after day 20 (especially in the Balmer lines), and a transient minimum is obtained around day 40–50; $\text{H}\beta$ disappears completely by that time. Afterwards absorption increases again. This purely *spectroscopic* behaviour between days 20 and 100 has no correspondance in the lightcurve, but in another spectroscopic phenomenon, the *Bochum event*: the fading of absorption in these lines correlates with spectral finestructure.

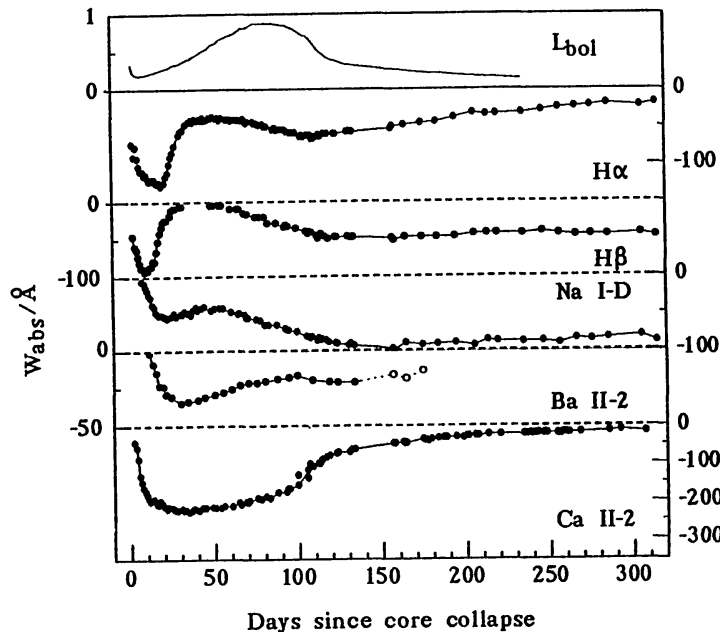


Fig. 4: Equivalent width W_{abs} for optical absorption troughs of the Balmer lines $H\alpha$ and $H\beta$, of Na I-D $\lambda 5890$, Ba II-2 $\lambda 6141$ and Ca II-2 $\lambda 8500$. Shown on top is the bolometric lightcurve. The Ba II-2 line fades away after day ~ 170 , open circles denote uncertain measurements. $H\beta$ disappears completely between days 35 and 50

In Na I-D absorption remains strong even beyond day 314 (cf. Spyromilio *et al.*, 1990). The same is true for $H\beta$ after its revival. While this behaviour is not surprising at $T \approx 5000$ K for Na I-D as a resonance line exhibiting a very large optical depth, the run of the $H\beta$ absorption is surprising as $H\alpha$ absorption fades away at the same time! By day 300, W_{α} is only half as large (~ 25 Å) as W_{β} (50 Å). However, the definition of $H\alpha$ absorption becomes worse with time due to the increasing strength of [O I] emission, veiling part of the $H\alpha$ absorption. The measured values in Fig. 4 should therefore be regarded only as a lower limit. Furthermore, weak blends in $H\beta$ could mimic too high an absorption strength at late times. However, no clear evidence for line-blending in the post-maximum phase is visible in the flux vs.time map of $H\beta$ (Hanuschik and Thimm, 1990). It is therefore not yet clear what the cause for the rather strange $H\alpha/H\beta$ ratio is.

4.2 Emission-line lightcurves

Emission-line lightcurves are even more complex than curves of absorption-line equivalent width because of the explicit dependence on the powering light source. Figure 5 shows the evolution of $H\alpha$ emission, with three maxima of emission: on day 5, around day 95 and around day 180, well in the

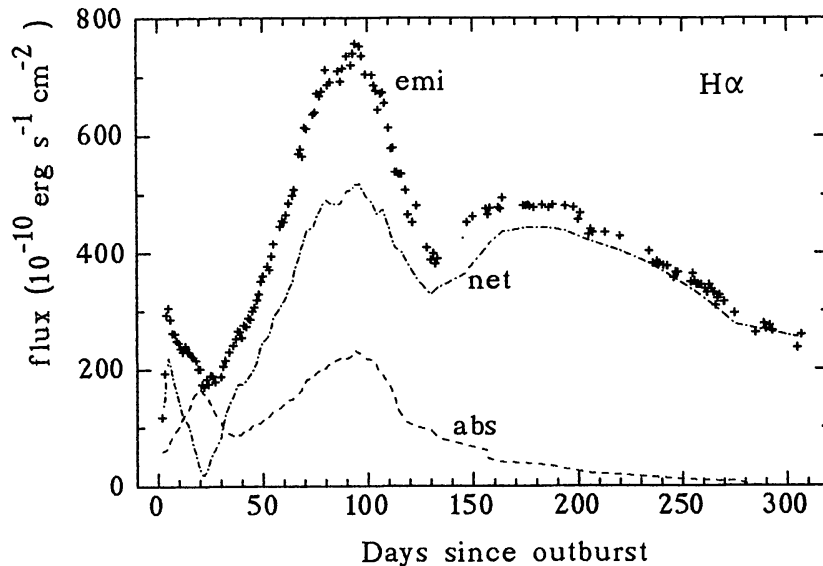


Fig. 5: Evolution of fluxes in $H\alpha$. Crosses denote the emission part of the P Cygni profile; the absorbed flux is marked by a broken, the net flux by a dash-dotted line. Fluxes are dereddened with $E_{B-V} = 0.16$ and can easily be transformed into luminosity by multiplying with 47.476 dex

exponential tail. As proposed by Thimm et al. (1989) and Phillips and Heathcote (1989), the early-time emission of $H\alpha$ can be understood in terms of powering by recombination (first maximum) and thermalized cobalt decay (second maximum). This is supported by the fact that both phases are separated by a short drop of the $H\alpha$ net emission to zero (Fig. 5). The third maximum could be due to the effect of an optically thick emitting $H\alpha$ disk ($\sim t^2$), combined with the exponential fall-off in the powering continuum ($\sim \exp[-t/111^d]$).

A similar maximum in the exponential phase, around day 200, occurs in the Ca II-2 $\lambda 8600$ emission (cf. Fig. 6) which runs parallel to the $H\alpha$ emission. In contrast, Na I-D emission fades away after the overall brightness maximum. The forbidden lines evolve differently: [Ca II] and [O I] emission approach their maximum well in the exponential tail, around day 250. There is no correlation with the lightcurve what is not surprising if these lines are collisionally excited. The increase in [Ca II] emission strength is roughly proportional to t^{-2} , as expected for an optically thick sphere.

4.3 Optical depth in forbidden lines

Even forbidden lines can become optically thick in expanding SN envelopes with their huge optical pathlengths. In a differentially expanding envelope, the emergent flux in a line is given, according to the Sobolev theory, by

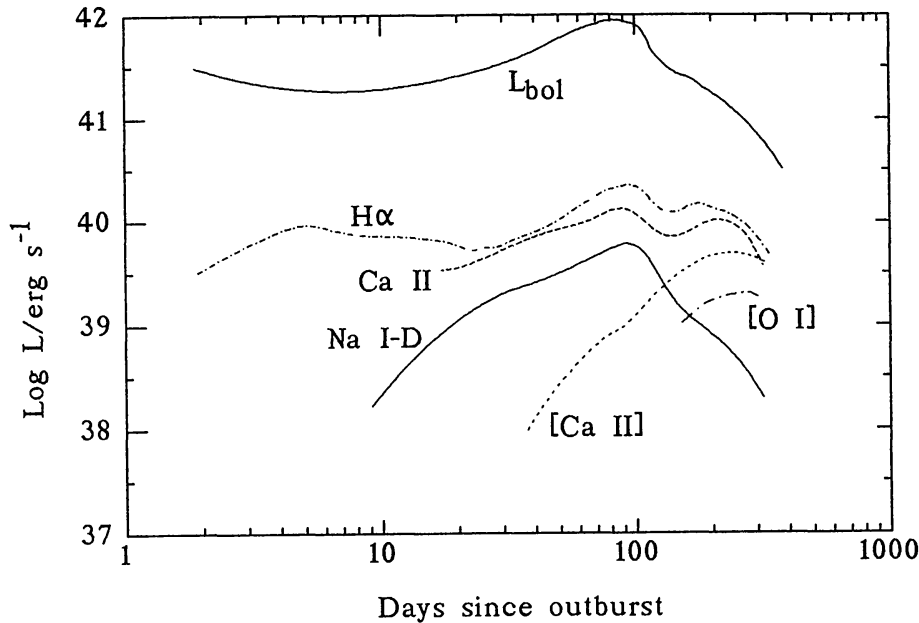


Fig. 6: Comparison of bolometric and emission-line luminosities in SN 1987A. For the evolution after day 314, compare, e.g., Phillips and Williams (1990) or Spyromilio *et al.* (1990). Here, the early-time evolution is emphasized by using a logarithmic timescale. Lines shown are $H\alpha$, Ca II $\lambda 8600$, Na I-D, [Ca II] $\lambda\lambda 7291/7323$ and [O I] $\lambda\lambda 6300/6363$

$I \sim \beta A_{ul} n_u$, with the escape probability $\beta = \tau^{-1} [1 - \exp(-\tau)]$, the number density in the upper state n_u and the Einstein coefficient for the transition investigated, A_{ul} . The optical depth τ_{Sob} is, for homologous expansion, proportional to $t \cdot n_1 \sim t^{-2}$. Then, the intensity ratio of a fine-structure doublet, such as [O I] $\lambda\lambda 6300/6363$ and [Ca II] $\lambda\lambda 7291/7323$, can be used to measure the optical depth in the line (see Phillips and Williams, 1990; Spyromilio *et al.*, 1990). The line ratio $I_1/I_2 = \beta_1 A_1 / \beta_2 A_2$ becomes

$$I_1/I_2 = [1 - \exp(-\tau_1)] / [1 - \exp(-\tau_2)] \quad (8)$$

which approaches unity in the optically thick limit, and A_1/A_2 in the optically thin limit.

Figure 7a shows that the optical depth in the primary [O I] component, calculated from (8), starts at $\tau_1 > 10$ and is still larger than 1 (≈ 2.5) on day 314. It falls off according to t^{-2} , as expected for expansive dilution. Evolution in the [Ca II] doublet is more puzzling (Fig. 7b). While this line seems to be optically thin when it first shows up, its optical depth *increases* to a value close to 2 around day 260. However, measuring the [Ca II] line ratio is more difficult than in [O I] as the separation is only 32 Å or 1300 km s⁻¹, less than the typical width of the main component, 2500 km s⁻¹ (cf. Hanuschik *et al.*, 1989). As optical depth effects play a role, the simple

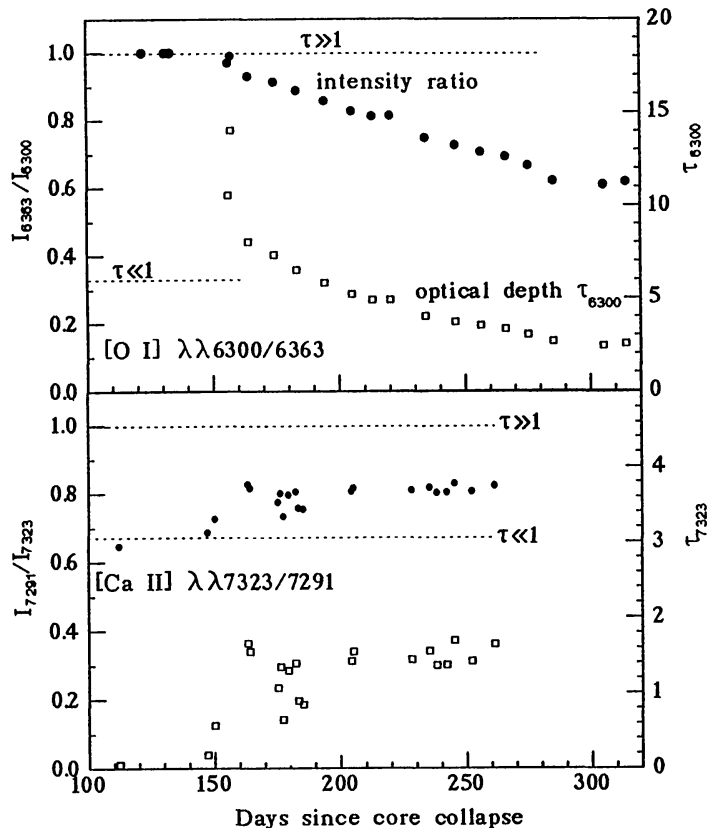


Fig. 7: Intensity ratio I_1/I_2 (full circles, left ordinate) and Sobolev optical depth τ_1 [open squares, right ordinate; cf. (8)] for the [O I] (top) and the [Ca II] (bottom) doublet in SN 1987A. As the [Ca II] doublet is rather narrow, only higher-resolution measurements at 3 Å from the Bochum telescope have been investigated, covering days 112–260. The line shows up, however, as early as on day 36 (Hanuschik *et al.*, 1989)

deblending technique described by Hanuschik *et al.* is probably not appropriate, and more sophisticated modelling is needed to treat the [Ca II] line profile properly.

5. Clumping and mixing

The simplest model for the kinematics of an expanding supernova envelope is the solution of the equation of continuity, i.e. homologous expansion:

$$v(r, t) = (r - r_0)/(t - t_0), \quad (9)$$

with r_0 the radius of the progenitor and t_0 the onset time of the expansion. However, there is evidence, e.g., for subsequent acceleration of the core (see above). Furthermore, it is well known that filaments in the youngest

galactic SN remnant, Cassiopeia A, move in a rather chaotic manner (Kirshner and Chevalier, 1977). Thus, turbulent mixing and clumping is expected to play an important role in the expansion of a supernova envelope (see Woosley *et al.*, 1988, and references therein). SN 1987A offers a first-row opportunity to study such mixing. Both indirect and direct evidence for mixing in SN 1987A exists.

5.1 Indirect evidence for mixing

The first evidence is the smooth transition in the bolometric lightcurve from powering by recombination into powering by radioactive decay, as well as the rather broad maximum (Fig. 3). Numerical models without mixing (e.g., Woosley, 1988, Fig. 15) fail to reproduce this smooth transition, but show a steep bump when all hydrogen has passed the photosphere and photons from the radioactive decay cannot yet diffuse into upper layers. Furthermore, their lightcurve maximum is rather steep and narrow. To better fit the observations, mixing-up of nickel bubbles, as well as mixing-down of hydrogen must be inferred (Pinto and Woosley, 1988).

The same kind of argumentation must be inferred to explain the early emergence of γ -rays from the ^{56}Co decay (Matz *et al.*, 1987). Contrary to the above described scenario that all decay energy was thermalized, a small fraction of γ -rays could obviously escape directly from the envelope, without being down-scattered and thermalized to optical photons, although the envelope was still optically thick at that time. Again, some ^{56}Co mixing-up must be assumed.

Thirdly, the high velocity ($\approx 4\,000\text{ km s}^{-1}$) observed in the wings of Co II and Ni II infrared lines (Aitken, 1988; Witteborn *et al.*, 1989) is an indication for mixing because unmixed core material moves at less than $1\,000\text{ km s}^{-1}$ according to model calculations (Woosley, 1988). Although electron scattering plays a role in broadening especially the red wing of the line profiles (see Woosley *et al.*, 1988, Fig. 12), the basic conclusion is valid that we are observing material freshly nucleosynthesized in the explosion at much higher velocity than expected from unmixed explosion models.

A fourth indirect evidence for mixing is the unusual strength of lines of Ba II ($\lambda\lambda 612, 4924, 4554$) and Sc II ($\lambda\lambda 6245, 5658, 5527$). These elements are produced by slow neutron capture (*s*-process) deep in the neutron-rich inner layers, not in the hydrogen envelope. Since they became visible in the optical spectrum as early as on day 10–20 (Hanuschik and Dachs, 1988), long before helium-rich layers appeared at the photosphere, again mixing-up of heavier elements is required.

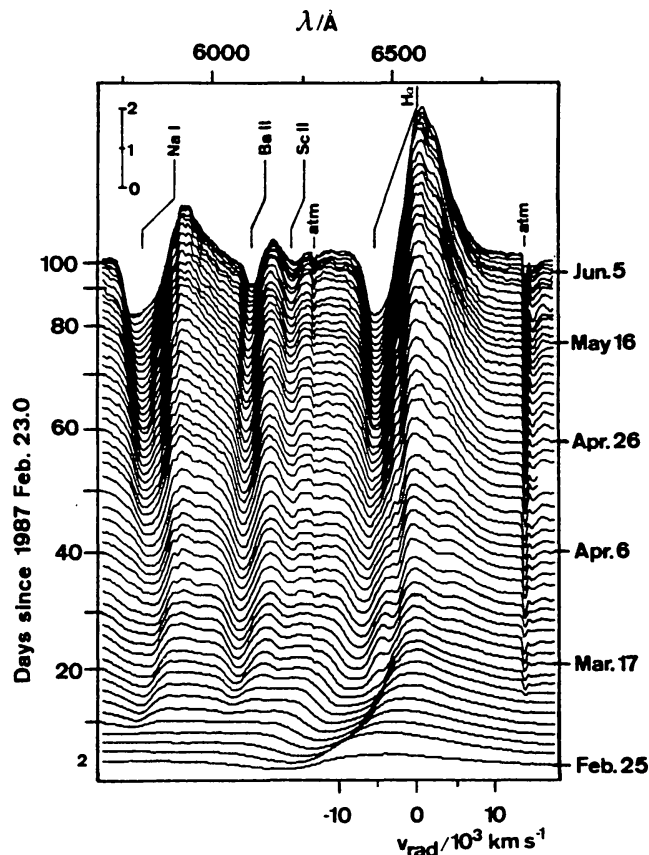


Fig. 8: The Bochum event in $H\alpha$ and Na I-D (Hanuschik *et al.*, 1988). In addition, the Ba II-2 $\lambda 6142$ and Sc II-28 $\lambda 6245$ lines are visible. To avoid crowding, only scans for every second day are shown

5.2 Direct evidence for mixing

The *Bochum event* is a transient spectroscopic finestructure feature in hydrogen and sodium lines, as documented by Hanuschik and Dachs (1987), Hanuschik *et al.* (1988), Phillips and Heathcote (1989) and Hanuschik and Thimm (1990). It was first detected as a satellite feature in the absorption trough of $H\alpha$ (Fig. 8), on day 19 = March 14, 1987. Slightly later, a similar structure evolved in the emission hump of this line, at the same (absolute) radial velocity. Related finestructure could be observed in $H\beta$ and Na I-D, as well as in infrared hydrogen lines (Phillips and Heathcote, 1989). The radial velocity of the finestructure in the $H\alpha$ trough was initially -5800 km s^{-1} , close to the photospheric value, and subsequently fell off to -2000 km s^{-1} . It disappeared during the transition to the exponential tail, around day ~ 120 .

The kinematic behaviour has been interpreted as evidence for a change of the excitation conditions of the matter penetrating the photosphere around

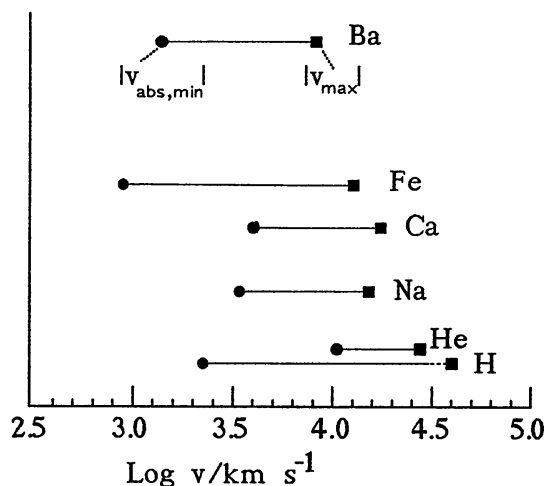


Fig. 9: Chemical stratification in the envelope. Indicated is the observed velocity spread of several species with prominent lines in the optical. See text for the definition of $v_{\text{abs, min}}$ and v_{max}

day 20 (Lucy, 1988; Hanuschik *et al.*, 1988); Phillips and Heathcote, 1989; Hanuschik and Thimm, 1990). This change is likely to be caused by mixed-up ^{56}Co bubbles or fingers. (Remember that direct evidence for cobalt at $\approx 4000 \text{ km s}^{-1}$ exists at later times, see above.) This suggestion is supported by recent detailed lightcurve modelling with ^{56}Co mixing (Shigeyama and Nomoto, 1990). The *Bochum event* thus is the earliest evidence for mixing in SN 1987A.

Another interesting diagnostic for the investigation of mixing processes is the search for chemical stratification from the kinematics of spectral lines. Such stratification should be rather pronounced in absence of mixing. In general, relating observed *radial* velocities to *true* velocities and radii is model dependent, except for two cases:

(1) The maximum blueshifted or redshifted (whatever is larger) radial velocity observed in a certain line, $|v_{\text{max}}|$, corresponds to (or sets a lower limit to) the highest outflow velocity of the species investigated, and hence of the *outer radius* of the corresponding shell.

(2) The velocity of the *inner boundary* of the shell is expected to become visible, in a trough velocity *vs.* time diagram (as, e.g., shown in Hanuschik and Schmidt-Kaler, 1989), as an asymptotic lower value, $|v_{\text{abs, min}}|$. Trough velocities are radial velocities of the flux minimum in an absorption trough.

For hydrogen, the maximum observed velocity is $|v_{\text{max}}| = 31000 \text{ km s}^{-1}$, as observed in $\text{H}\alpha$ on day 1.8 (Hanuschik and Dachs, 1987). The lowest hydrogen velocity is seen in $\text{H}\gamma$, $|v_{\text{abs, min}}| = 2240 \text{ km s}^{-1}$, reached asymptotically around day 170 (Hanuschik *et al.*, 1991). No lower trough velocity has been observed in hydrogen lines so far. It is therefore reasonable to conclude that hydrogen is present in the envelope from at least 2240 up to at least 31000 km s^{-1} .

In a similar way, upper and lower boundaries for He, Na, Ca, Fe and Ba zones can be derived from optical lines (Fig. 9). Obviously, heavier elements, even iron and barium, are found far out in what in unmixed

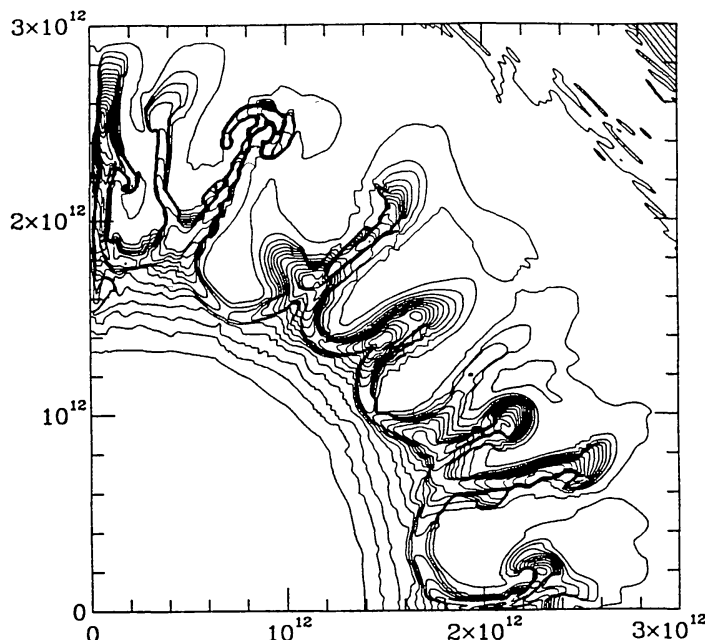


Fig. 10: Model calculation showing Rayleigh–Taylor instabilities and mixing 2.7 hrs after explosion (Müller *et al.*, 1989). Density contours are shown at 5 % spacing

models is the pure hydrogen envelope, i.e. at velocities of up to 10^4 km s^{-1} . For comparison, in unmixed models (Woosley, 1988) helium and calcium should mainly show up at $\approx 10^3$ km s^{-1} .

A number of model calculations exist (e.g., Müller *et al.*, 1989, Arnett *et al.*, 1989, and references therein) that predict turbulent mixing by Rayleigh–Taylor instabilities at the He–H boundary, a few hours after shock-breakout (Fig. 10). A few mushroom-like bubbles may have reached 4 000 km s^{-1} in the course of this early-time mixing. A second phase with mixing could have occurred later, after ≈ 10 days, when a substantial amount of energy had been deposited in the inner layers by the onset of the Ni–Co decay.

5.3 Clumping

Closely related to mixing processes is clumping, i.e. small-scale density, not necessarily velocity gradients. These clumps are directly visible in the line profiles as bumps or wiggles at sufficiently high resolution and S/N. Because their radial velocity is expected to be constant with time, they can easily be discerned from the *Bochum event* which is variable in radial velocity.

Clumping in SN 1987A line profiles was observed by Stathakis and Cannon (1988) in December 1987 and thereafter, and by Thimm (1989,

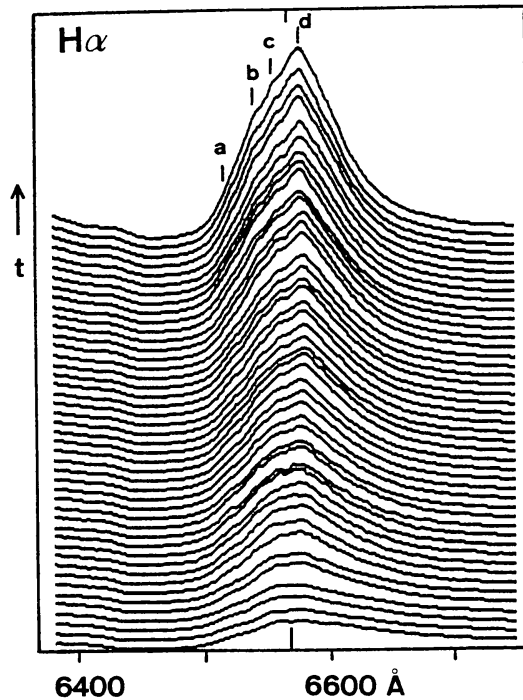


Fig. 11: Bumps and clumping. All $H\alpha$ profiles measured between days 111 and 260 at 3 \AA resolution are plotted, with the fluxes being normalized to their value at 6875 \AA . Four bumps (a-d) appear around day 160 (cf. Fig. 12)

private communication). It appears as finestructure humps on top of the envelope emission in $[\text{O I}] \lambda\lambda 6300/63$, $[\text{Ca II}] \lambda\lambda 7291/7324$ and $H\alpha$. These humps have a typical width of $\approx 100 \text{ km s}^{-1}$ (FWHM).

At lower resolution ($3 \text{ \AA} \hat{=} 140 \text{ km s}^{-1}$), the high-S/N profiles of $H\alpha$ obtained with the Bochum telescope show the onset of clumpy finestructure around day 160 ± 10 (Figs. 11, 12). There are four bumps, constant in radial velocity at -2000 , -900 , -200 , and $+500 \text{ km s}^{-1}$, persistent through day 300. Their width is $300\text{--}400 \text{ km s}^{-1}$. These bumps are quite pronounced and stronger than those visible on high-resolution spectra, but they appear on the blue side of the emission profile, in the steep flank, and therefore are barely visible on single spectra. Only an extensive time record, together with contrast enhancement (Fig. 12), makes them stand out clearly.

We can exclude the possibility that these clumps were existing before — hidden below the photosphere —, because the photospheric velocity on day 160 is only 660 km s^{-1} , while the lower boundary of the hydrogen shell is $\approx 2200 \text{ km s}^{-1}$, so that the bulk of the hydrogen had already passed the photosphere around day 50. It is therefore likely that *we observe, on day 160, the onset of clumping in the hydrogen envelope.*

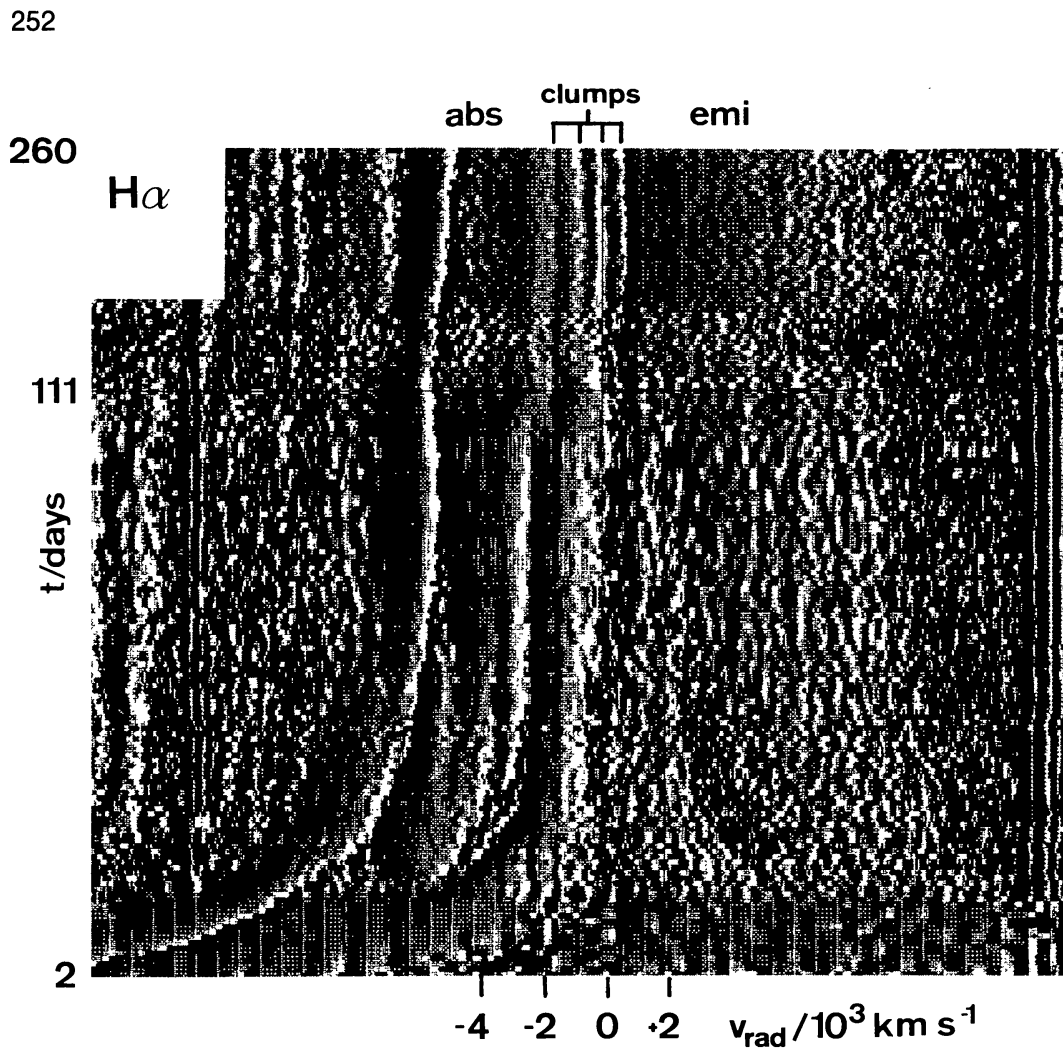


Fig. 12: Grey-scaled plot of the $H\alpha$ fine-structure. Shown in this plot is essentially the second derivative of fluxes, resulting in considerable contrast enhancement of faint flux gradient changes. Note that scaling of the time axis is compressed after day 111 (one spectrum per ≈ 3 days on the average). The four bumps indicating clumping appear as straight lines after day 160, while the Bochum event shows up as complex features between day 20 and 120, variable in radial velocity.

6. History of the progenitor: the circumstellar medium

6.1 The CSM shell

According to evolutionary models (e.g., Saio *et al.*, 1988; Woosley *et al.*, 1988), a $20 M_{\odot}$ star loses a significant amount of mass during its red supergiant phase in form of a dense, slow ($\approx 10 \text{ km s}^{-1}$) *rsg* stellar wind. When Sk -69°202 turned into its blue supergiant phase, it started to develop a fast (10^3 km s^{-1}), low density *bsg* stellar wind. This *bsg* wind blew a cavity into the preexisting *rsg* wind and developed a shock front marking

the *rsg-bsg* wind boundary. Remnants of these fossil stellar winds, and especially the density-enhanced shock zone, are expected to constitute the circumstellar medium (CSM) surrounding SN 1987A.

The CSM shock zone was struck by the EUV flash from shock break-out in SN 1987A and began to fluoresce in nebular emission lines which became visible as soon as the envelope emission faded. It is important to realize that the signal in these lines comes from the shock zone itself and not from the expanding explosion light, like in the case of the famous light echoes. It is therefore geometrically stationary, apart from light-travel time and recombination effects within the shock zone itself. The narrow emission lines were first detected in the UV (Fransson *et al.*, 1989), later also in the optical (Wampler and Richichi, 1989). From the [O III] lines, a temperature of 55 000 K is derived for the excited shock zone in December 1989. Their peak radial velocity, $286.3 \pm 0.8 \text{ km s}^{-1}$, is at present the best estimate we have for the system velocity of Sk -69°202/SN 1987A. The resolved width at H α (thermal plus kinematic) is $25.9 \pm 0.3 \text{ km s}^{-1}$, the velocity gradient, measured across the spatially resolved H α line, is only 3–6 km s^{-1} (Wood and Faulkner, 1989; Hanuschik, 1990c). The expansion velocity of the shell cannot be larger than $\sim 10 \text{ km s}^{-1}$, otherwise the H α line would be broadened stronger.

The spatial extent of the shock zone is 1.6" by 1.1" with a ring-like geometry, as seen on NTT images taken at 0.5" seeing in December 1989 (Wampler *et al.*, 1990). These parameters are confirmed by the recent HST image. We thus see a flattened ellipsoid, or a flattened torus, or a circular ring, centred on SN 1987A at distance $7 \cdot 10^{17} \text{ cm}$ or 0.7 lightyears. However, one has to be careful in translating these observations into the geometry of the shock zone because apart from aspect effects both light travel time and recombination time play a role (Fransson *et al.* 1989; Fransson and Lundqvist, 1989).

The apparent asphericity of the CSM shell is remarkable, no matter whether it is, in reality, a flattened ellipsoid (then the ring-like appearance is due to limb-brightening as in the case of a planetary nebula) or a symmetrical, but inclined torus (then inclination must be 45°): in either case, this asphericity hints towards a *non-spherical outflow*, most likely due to rapid rotation of the blue supergiant. One should expect that this asymmetry might also be also visible in the *ejecta* of SN 1987A. Indeed, there is multiple evidence for a non-spherically symmetric explosion: Polarimetric observations (Schwarz and Mundt, 1987; Cropper *et al.*, 1988) reveal intrinsic continuum polarization of the envelope of 0.28 %, as early as on day 12. This value of polarization would result, according to models of Shapiro and Sutherland (1982), either from an oblate spheroid with axis ratio $\mu = 0.77$, or from an prolate spheroid with $\mu = 0.70$. Furthermore, direct speckle imaging (Karovska *et al.*, 1989) indicates an axis ratio of the supernova

envelope of 0.6 at $H\alpha$ on days 95–98, and less elongation at other wavelengths. The elongated axis is at position angle 20 – 30° . For comparison, the NTT and HST images show the major axis of the CSM shell at $\sim 80^\circ$.

We can conclude that SN 1987A is the first one to prove that SNe do not necessarily explode in a nice, easy-to-model spherical symmetric way. Furthermore, as the observations in the CSM also suggest asphericity in the fossil outflow from the progenitor star, one can conclude that both asymmetries, of the outflow and of the explosion, arise from rotation of the star.

6.2 Other CSM components

The $1.6''$ by $1.1''$ ring is the most prominent, but not the only CSM feature yet seen. On high-resolution spectra taken in September 1989, substructure of the CSM $H\alpha$ feature was detected (Hanuschik, 1990c), in form of a very narrow (unresolved at 10 km s^{-1} resolution) source at $2.1''$ (1.7 lightyears) projected distance NW of the supernova (Fig. 13). As finestructure broadening of $H\alpha$ contributes about 6 km s^{-1} (Dyson and Meaburn, 1971) to any observed width, thermal broadening must be very small, corresponding to less than 1400 K . This $H\alpha$ feature could arise from a condensation of gas and dust, visible as an arc on the NTT images (Wampler *et al.*, 1990) extending to the NW of the supernova. Recent images of the area (Crofts, 1990; Elias, 1990) show several knots in $H\alpha$ and He I 1.083μ , one of them coincident with the spectroscopic $H\alpha$ blob. These condensations probably are remnants of dust shells expelled by the progenitor star in its *rsg* phase and now are excited to fluorescence, like the shock zone, by the EUV flash.

Finally, the recent detection of the onset of radio emission in July 1990 (Turtle *et al.*, 1990) seems to herald a revival of the fading envelope of SN 1987A by interaction of the outermost debris of the explosion, moving at $40\,000 \text{ km s}^{-1}$, with the fossil CSM. These layers now are 0.5 lightyears away from the core of the explosion, still well within the *bsg* stellar wind zone. Therefore their brightening is most likely due to the collision with a cloud within this innermost CSM region. From the rising time of the signal, a size of $5 \cdot 10^{16} \text{ cm}$ or 20 lightdays can be inferred for this cloud (Chevalier, 1990). Alternatively, the radio signal could mark the onset of pulsar activity.

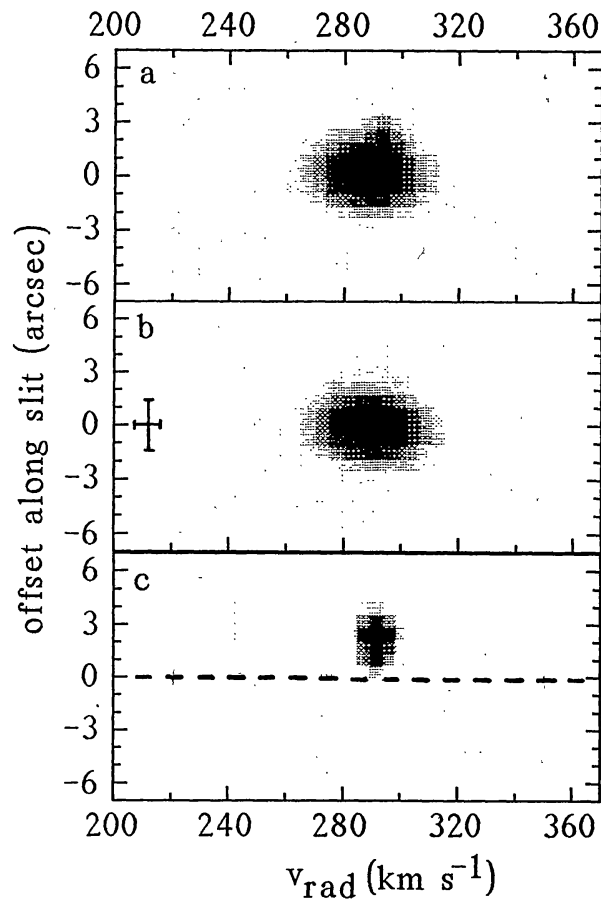


Fig. 13: Spectrum of the CSM $H\alpha$ component from the vicinity of SN 1987A (cf. Hanuschik, 1990c). **13a:** The $H\alpha$ line after subtraction of supernova and H II-region emission. **13b:** Primary component arising from the CSM shell. **13c:** The $H\alpha$ blob, obtained by subtraction of Fig. 13b from Fig. 13a. The spectral narrowness, as well as the offset from the supernova position (indicated by a broken line) is clearly visible. Intensity scaling is the same in all three images. Spectral as well as spatial resolution is indicated in Fig. 13b

7. Conclusions: old and new questions

Supernova 1987A in the LMC has answered many old questions and risen many new ones. The pioneering idea of Baade and Zwicky (1934) that supernovae (of type II) gain their energy from the gravitative collapse of a massive star has been proven. But the first supernova ever with a certain progenitor identification demonstrated that these stars can finish their ordinary life not only as red, but also as blue supergiants. The exploded blue supergiant Sk -69°202 proved, in a certain sense, the suggestion of Shklovskii (1984) that in irregular galaxies, like the LMC, type-II SNe are missed because they are fainter. In fact, the lower metallicity, together with the specific ZAMS mass, mass loss and semi-convection, seem to be the

determining parameters for the final state of the massive star at explosion (e.g., Woosley *et al.*, 1988). Thus evolutionary calculations for this part of the HRD have become attractive again.

The same is true for the field of supernova statistics: only 1 type-1987A event for every 50 normal type-II's would be observed if intrinsically both types are equally frequent.

The neutrino signal also confirmed another prediction, viz. that the energy gained in the collapse must be radiated away mainly in form of neutrinos. But no satisfying and consistent answer exists to the question: what happened 4.6 hrs before t_0 in the Mt. Blanc neutrino detector (Aglietta *et al.*, 1987)? Also, because the information contained in 19 officially accepted neutrinos is quite limited, we have virtually nothing learnt about how a supernova explodes, i.e. how a small fraction of the collapse energy (1 %) is transferred into explosion energy of the envelope.

Another important result from SN 1987A is the confirmation that SNe indeed produce heavy elements. Specifically, the exact amount of ^{56}Ni produced in the shock could be measured by comparison to the lightcurve and by analyzing the IR lines of this species.

SN 1987A has also demonstrated that mixing and clumping are important processes in the very early evolution of the expanding envelope, and that asphericity of the envelope is an observational fact that has to be considered in future model calculations.

This supernova will remain a highly interesting object in the future. Some prospective highlights are the manifestation of a central pulsar and the radio and X-rays from the interaction of the envelope with the fossil CSM. If the young remnant of SN 1987A evolves similarly to SN 1054, the remnant of which we observe in the Crab nebula, it will possess a brightness of $\approx 15^m$ and a diameter of 12 arcseconds in the year 2926, then being even more impressive than presently.

References

- Aglietta, M. et al.: 1987, *Europhys. Lett.* **3**, 1315/1321
 Aitken, D. K.: 1988, *Proc. Astron. Soc. Aust.* **7**, 462
 Arnett, W. D.: 1989, *Astrophys. J.* **343**, 834
 Arnett, W. D., Bahcall, J.N., Kirshner, R.P., Woosley, S.E.: 1989, *Annu. Rev. Astron. Astrophys.* **27**, 629
 Baade, W., Zwicky, F.: 1934, *Proc. Nat. Acad. Sci. US* **20**, 254
 Barbon, R., Capellaro, E., Turatto, M.: 1989, *Astron. Astrophys. Suppl.* **81**, 421
 Bionta, R.M., Blewitt, G., Bratton, C., Caspar, D.: 1987, *Phys. Rev. Lett.* **58**, 1494
 Bouchet, P.: 1990, in *Proc. ESO/EIPC Workshop "SN1987A and other supernovae"*, I. J. Danziger (ed.), ESO, Garching, 1990 (*in press*)
 Bouchet, P., Danziger, I.J., Lucy, L.B.: 1989a, *IAU Circ.* 4933

- Bouchet, P., Moneti, A., Slezak, E., Le Bertre, T., Manfroid, J.: 1989b, *Astron. Astrophys. Suppl.* **80**, 379
- Bouchet, P., Phillips, M.M., Suntzeff, N.B., Gouiffes, C., Hanuschik, R.W., Wooden, D.: 1990, *Astron. Astrophys.* (*submitted*)
- Burrows, A.: 1988, *Astrophys. J.* **334**, 891
- Chevalier, R.A.: 1990, in *Proc. ESO/EIPC Workshop "SN1987A and other supernovae"*, I.J. Danziger (ed.), ESO, Garching, 1990 (*in press*)
- Cropper, M., Bailey, J., McCowage, J., Cannon, R.D., Couch, W.J., Walsh, J.R., Strade, J.O., Freeman, F.: 1988, *Mon. Not. R. Astron. Soc.* **231**, 695
- Crotts, A.P.S.: 1990, in *Proc. ESO/EIPC Workshop "SN1987A and other supernovae"*, I.J. Danziger (ed.), ESO, Garching, 1990 (*in press*)
- Danziger, I.J. (ed.): 1987, *Proc. ESO Workshop on the SN1987A*, ESO, Garching
- Danziger, I.J. (ed.): 1990, *Proc. ESO/EIPC Workshop "SN1987A and other supernovae"*, ESO, Garching, 1990 (*in press*)
- Dopita, M.: 1988, *Space Sci. Rev.* **46**, 225
- Dopita, M. et al.: 1988, *Astron. J.* **95**, 1717
- Dyson, J.E., Meaburn, J.: 1971, *Astron. Astrophys.* **12**, 219
- Elias, J.H.: 1990, in *Proc. ESO/EIPC Workshop "SN1987A and other supernovae"*, I.J. Danziger (ed.), ESO, Garching, 1990 (*in press*)
- Filippenko, A.: 1990, in *Proc. ESO/EIPC Workshop "SN1987A and other supernovae"*, I.J. Danziger (ed.), ESO, Garching, 1990 (*in press*)
- Fransson, C., Cassatella, A., Gilmozzi, R., Kirshner, R.P., Panagia, N., Sonneborn, G., Wamsteker, W.: 1989, *Astrophys. J.* **336**, 449
- Fransson, C., Lundqvist, P.: 1989, *Astrophys. J.* **341**, L59
- González, R., Wamsteker, W., Gilmozzi, R., Walborn, N., Lauberts, A.: 1987, in *ESO Workshop on the SN1987A*, I.J. Danziger (ed.), ESO, Garching, p. 33
- Greco, M. (ed.): 1988, *Proc. Workshop "SN 1987A, One Year Later"*, Edition Frontières, Gif-sur-Yvette
- Hanuschik, R.W.: 1989, *Rev. Mod. Astron.* **2**, 148
- Hanuschik, R.W.: 1990a, in *Proc. Xth Santa Cruz Summer Workshop in Astronomy and Astrophysics "Supernovae"*, S. Woosley (ed.), Springer, Heidelberg (*in press*)
- Hanuschik, R.W.: 1990b, in *Proc. ESO/EIPC Workshop "SN1987A and other supernovae"*, I.J. Danziger (ed.), ESO, Garching, 1990 (*in press*)
- Hanuschik, R.W.: 1990c, *Astron. Astrophys.* **237**, 12
- Hanuschik, R.W., Dachs, J.: 1987, *Astron. Astrophys.* **182**, L29
- Hanuschik, R.W., Dachs, J.: 1988, *Astron. Astrophys.* **205**, 135
- Hanuschik, R.W., Schmidt-Kaler, Th.: 1989, *Mon. Not. R. Astron. Soc.* **241**, 347
- Hanuschik, R.W., Thimm, G.J.: 1990, *Astron. Astrophys.* **231**, 77
- Hanuschik, R.W., Thimm, G.J., Dachs, J.: 1988, *Mon. Not. R. Astron. Soc.* **234**, 41P
- Hanuschik, R.W., Thimm, G.J., Seidensticker, K.J.: 1989, *Astron. Astrophys.* **220**, 153
- Hanuschik, R.W., Gochermann, J., Kimeswenger, S., Poetzel, R., Schnur, G.F.O., Weger, M.: 1991, *in preparation*
- Haupt, W., Desjardins, R., Maitzen, H.M., Rudolph, R., Schlosser, W., Schmidt-Kaler, Th., Tüg, H.: 1976, *Astron. Astrophys.* **50**, 85
- Hillebrandt, W., Höflich, P.: 1989, *Rep. Prog. Phys.* **52**, 1421
- Hirata, K. et al.: 1987, *Phys. Rev. Lett.* **58**, 1490

- Isserstedt, J.: 1975, *Astron. Astrophys. Suppl.* **19**, 259
- Kafatos, M., Michalitsianos, A. (eds.): 1988, *Proc. 4th George Mason University Workshop in Astrophysics "Supernova 1987A in the LMC"*, Cambridge University Press, Cambridge
- Kare, J.T. et al.: 1989, *Rev. Sci. Instrum.* **59**, 1021
- Karovska, M., Koechlin, L., Nisenson, P., Papaliolios, C., Standley, C.: 1989, *Astrophys. J.* **340**, 435
- Kirshner, R.P., Chevalier, R.A.: 1977, *Astrophys. J.* **218**, 142
- Kirshner, R.P., Sonneborn, G., Grenshaw, D.M., Nassiopoulos, G.E.: 1987, *Astrophys. J.* **320**, 602
- Lucy, L.: 1988, in *4th George Mason University Workshop in Astrophysics "Supernova 1987A in the LMC"*, M. Kafatos and A. Michalitsianos (eds.), Cambridge University Press, Cambridge, p. 323
- Matz, S.M., Share, G.H., Leising, M.D., Chupp, E.L., Vestrand, W.T., Purcell, W.R., Strickman, M.S., Reppin, C.: 1988, *Nature* **331**, 416
- McCray, R.: 1989, in *Proc. Yellow Mountain Summer School "Structure and Evolution of Galaxies"*, L.-Z. Fang (ed.), World Science, Singapore, p. 8
- Menzies, J. et al.: 1987, *Mon. Not. R. Astron. Soc.* **227**, 39P
- Miller, D.L., Branch, D.: 1990, *Astron. J.* **100**, 530
- Müller, E., Hillebrandt, W., Orio, M., Höflich, P., Mönchmeyer, R., Arnett, D., Fryxell, B.: 1989, in *Proc. 5th Workshop on Nuclear Astrophysics (Schloß Ringberg)*, W. Hillebrandt und E. Müller (eds.), MPA/P1, p. 103
- Perlmutter, S.: 1990, in *Proc. ESO/EIPC Workshop "SN1987A and other supernovae"*, I. J. Danziger (ed.), ESO, Garching, 1990 (*in press*)
- Phillips, M.M.: 1988, *Proc. Astron. Soc. Aust.* **7**, 11
- Phillips, M.M., Heathcote, S.R.: 1989, *Publ. Astron. Soc. Pacific* **101**, 137
- Phillips, M.M., Williams, R.E.: 1990, in *Proc. Xth Santa Cruz Summer Workshop in Astronomy and Astrophysics "Supernovae"*, S. Woosley (ed.), Springer, Heidelberg (*in press*)
- Pinto, P.A., Woosley, S.E.: 1988, *Astrophys. J.* **329**, 820
- Saio, H., Kato, M., Nomoto, K.: 1988, *Astrophys. J.* **331**, 388
- Sanduleak, N.: 1969, *CTIO contribution No. 89*, Cerro Tololo Interamerican Observatory, La Serena, Chile
- Schwarz, H.E., Mundt, R.: 1987, *Astron. Astrophys.* **177**, L4
- Shapiro, P.R., Sutherland, P.G.: 1982, *Astrophys. J.* **263**, 902
- Shigeyama, T., Nomoto, K.: 1990, *Astrophys. J.* **360**, 242
- Shklovskii, I.S.: 1984, *Pis'ma Astron. Zh.* **10**, 723 (english translation: *Sov. Astron. Lett.* **10**, 302)
- Spyromilio, J., Stathakis, R.A., Cannon, R.D., Waterman, L., Couch, W.J., Dopita, M. A.: 1990, *submitted to Mon. Not. R. Astron. Soc.*
- Stathakis, R., Cannon, R.: 1988, *AAO Newsl.* no. 45
- Suntzeff, N., Bouchet, P.: 1990, *Astron. J.* **99**, 650
- Thimm, G.J., Hanuschik, R.W., Schmidt-Kaler, Th.: 1989, *Mon. Not. R. Astron. Soc.* **238**, 15P
- Tüg, H.: 1980a, *Astron. Astrophys. Suppl.* **39**, 67
- Tüg, H.: 1980b, *Astron. Astrophys.* **82**, 195
- Turtle, A.J., Campbell-Wilson, D., Manchester, R.N., Staveley-Smith, L., Kesteven, M.J.: 1990, *IAU Circ.* 5086
- Walborn, N.R., Prévot, M.L., Prévot, L., Wamsteker, W., González, R., Gilmozzi, R., Fitzpatrick, E.L.: 1989, *Astron. Astrophys.* **219**, 229
- Walker, A.R., Suntzeff, N.B.: 1990, *Publ. Astron. Soc. Pac.* **102**, 131

- Wampler, E.J., Richichi, A.: 1989, *Astron. Astrophys.* **217**, 31
- Wampler, J., Wang, L., Baade, D., Banse, K., D'Odorico, S., Gouiffes, C., Tarengi, M.: 1990 (*preprint*)
- Wamsteker, W., Panagia, N., Barylak, M., Cassatella, A., Clavel, J., Gilmozzi, R., Gry, C., Lloyd, C., van Santvoort, J., Talavera, A.: 1987, *Astron. Astrophys.* **177**, L21
- Whitelock, P.A. et al.: 1988, *Mon. Not. R. Astron. Soc.* **234**, 50P
- Witteborn, F.C. et al.: 1989, *Astrophys. J. (Letters)* **338**, L9
- Wood, P.R., Faulkner, D.J.: 1989, *IAU Circ.* 4739
- Wosley, S.E.: 1988, *Astrophys. J.* **330**, 218
- Wosley, S.E., Pinto, P.A., Weaver, T.A.: 1988, *Proc. Astron. Soc. Aust.* **7**, p. 355
- Wosley, S.: 1990, *Proc. Xth Santa Cruz Summer Workshop in Astronomy and Astrophysics "Supernovae"*, Springer, Heidelberg, in press